

Electronic supplementary information

**Amplifying the excited state chirality through self-assembly  
and subsequent enhancement via plasmonic silver nanowires**

Kuo Fu,<sup>a,b,†</sup> Xue Jin,<sup>b,†</sup> Minghao Zhou,<sup>b</sup> Kai Ma,<sup>b</sup> Pengfei Duan<sup>\*,b</sup> and Zhen-Qiang Yu<sup>\*,a</sup>

<sup>a</sup> College of Chemistry and Environmental Engineering, Low dimensional Materials  
Genome Initiative Shenzhen University 1066 Xueyuan Avenue, Nanshan, Shenzhen  
518055, P.R. China. E-mail: zqyu@szu.edu.cn

<sup>b</sup> CAS Center for Excellence in Nanoscience, CAS Key Laboratory of Nanosystem and  
Hierarchical Fabrication, National Center for Nanoscience and Technology (NCNST),  
No. 11 ZhongGuanCun BeiYiTiao, Beijing 100190, P. R. China.

Corresponding Authors

\*E-mail (Z. Yu): zqyu@szu.edu.cn.

\*E-mail (P. Duan): duanpf@nanoctr.cn.

**Characterization.** UV-vis spectra, fluorescence spectra and CD spectra were obtained using a Hitachi UH4150, Hitachi F-4600 and JASCO 1500 spectrometers, respectively. CPL measurements were performed with JASCO CPL-200 and JASCO CPL-300 spectrometer. Fluorescent microscopy was recorded on the Olympus X83 using high-pressure mercury lamp as excitation source for fluorescent images. Scanning electron microscopy (SEM) was performed on a Hitachi S-4800 FE-SEM with an accelerating voltage of 10 kV. Before SEM measurements, the samples on silicon wafers were coated with a thin layer of Au to increase the contrast. The samples were suspended on carbon-coated Cu grids, for transmission electron microscope (TEM) measurement on a T20 electron microscope (100 KV). Fourier transform infrared spectra FT-IR studies were performed with a JASCO FTIR-660 spectrometer. Dynamic light scattering (DLS) studies were performed with a Zetasizer Nano ZS ZEN3600. The fluorescence lifetime measurements were recorded on a NanoLOG-TCSPC fluorescence spectrometer using time-correlated single photon counting.

**Materials.** Anhydrous ethylene glycol (EG, 99.8%) was purchased MARED, Silver nitrate and polyvinyl pyr-rolidone (PVP,  $M_w = 55000$ ) were purchased from alfa-aesar (China) chemical Co., Ltd. Sodium chloride was purchased from Beijing chemical works and Other organic solvents was purchased from Beijing Chemical Reagent Company. (11bR)-2,6-Di-9-anthracenyl-8,9,10,11,12,13,14,15-octahydro-4-hydroxy-4-oxide-dinaphtho[2,1-d:1',2'-f] [1,3,2] dioxaphosphopin (*R*-OPAn) were purchased from Daicel Chiral Compounds (Shang Hai) without further purification.

**Synthesis of AgNWs.** PVP coated AgNWs were synthesized by the reduction of AgNO<sub>3</sub> using EG. First, 5 mL of a 2.2 mg/mL sodium chloride solution was prepared, and 1.6 g of PVP was dissolved in 25 mL of EG and heated and stirred in a 120 °C oil bath. After the PVP was completely dissolved, 1.5 mL of a sodium chloride solution ( $n_{\text{Cl}}:n_{\text{Ag}} = 3/85$ ) was added to the PVP EG solution to form a homogeneous mixed solution. Thereafter, 0.27 g of AgNO<sub>3</sub> was dissolved in 15 mL of EG and stirred to dissolve. After the AgNO<sub>3</sub> was completely dissolved, it was slowly added dropwise to the above mixed solution, and then heated in an oil bath at 160 °C for 7 hours. After the reaction was completed, a gray solution was obtained, and after naturally cooling to room temperature, the final product was washed multiple times by ethanol to remove ethylene glycol and excess surfactant PVP, and the AgNWs was subsequently stored at 4 °C.

**Fabrication of R-OPAn/AgNWs composite.** A certain mass of R-OPAn molecules were dissolved in ethanol, respectively. The sample concentration of R-OPAn was  $2.5 \times 10^{-3}$  M, and the concentration of silver nanowires was 2 mg/ml. The 200  $\mu$ l of the above mother liquor was separately taken out and different volumes of silver nanowire solution were added to prepare a composite having a mass ratio  $m_{\text{AgNWs}}/m_{\text{R-OPAn}}$  of 0 to 3.5, which was stirred overnight. (The final volume is 1ml to ensure the molecular concentration is unchange).

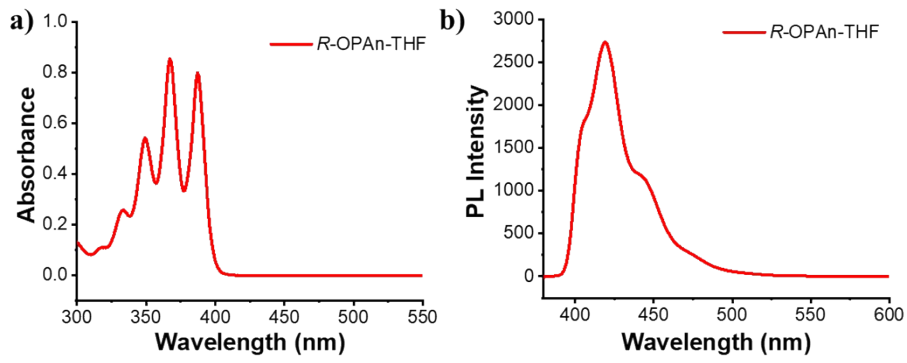


**Fig. S1** UV-vis spectra (a) and Fluorescence spectra (b) of *R*-OPAn dissolved in THF ( $[R\text{-OPAn}] = 5 \times 10^{-4}$  M,  $\lambda_{\text{ex}} = 360$  nm).

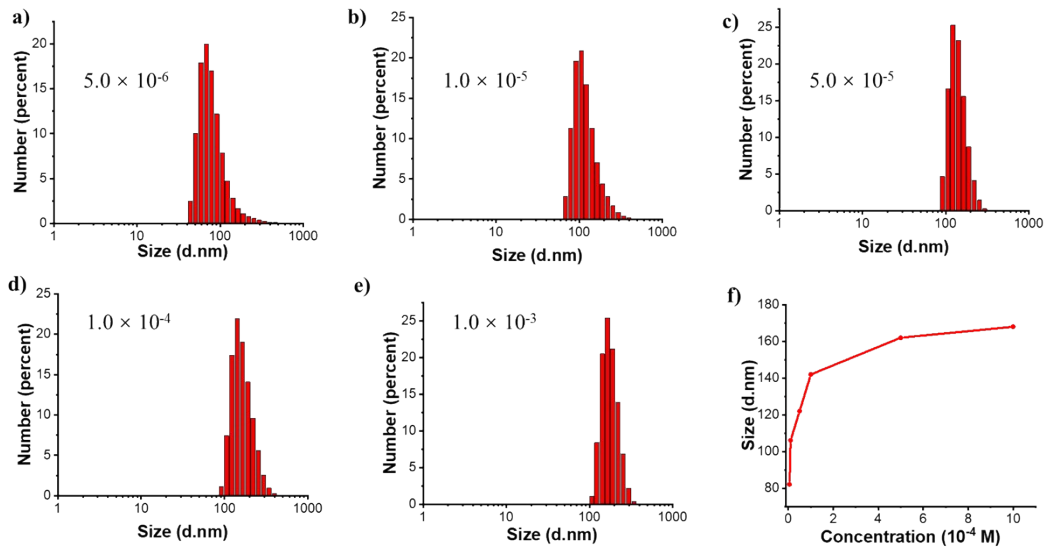


**Fig. S2** (a) ~ (e) Dynamic light scattering data of different concentration of *R*-OPAn-NPs in ethanol. The corresponding concentration of *R*-OPAn is  $5 \times 10^{-6}$ ,  $1 \times 10^{-5}$ ,  $5 \times 10^{-5}$ ,  $1 \times 10^{-4}$ ,  $1 \times 10^{-3}$  M. (f) The nanoparticle size of different concentrations of *R*-OPAn-NPs in ethanol.

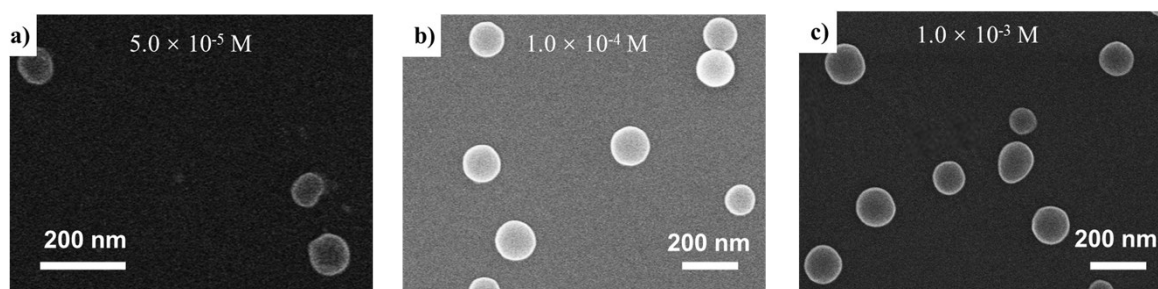


**Fig. S3** (a) ~ (c) The SEM image of different concentrations of *R*-OPAn-NPs in ethanol. The corresponding concentration of *R*-OPAn-NPs is  $5 \times 10^{-5}$ ,  $1 \times 10^{-4}$ ,  $1 \times 10^{-3}$  M.

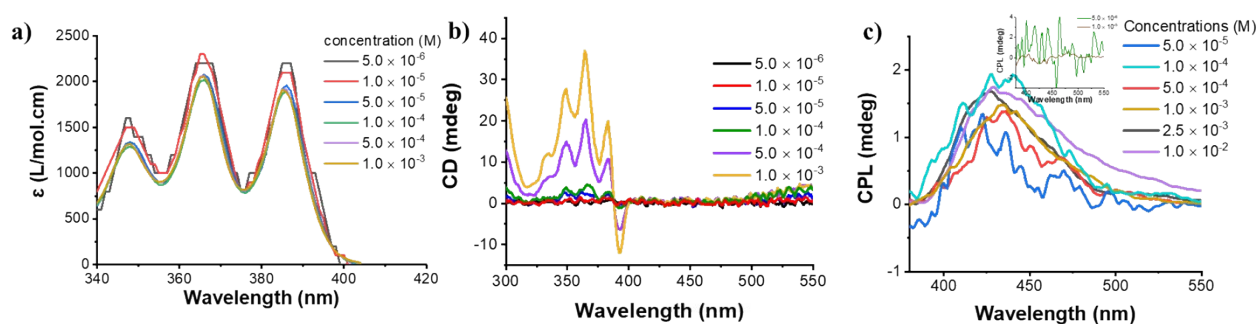


**Fig. S4** (a) UV-vis spectra spectra of *R*-OPAn-NPs in different concentrations. CD spectra (b) and CPL spectra (c) of different concentrations of *R*-OPAn in ethanol, the concentration of the samples:  $5 \times 10^{-5}$ ,  $10^{-4}$ ,  $5 \times 10^{-4}$ ,  $1.0 \times 10^{-3}$ ,  $2.5 \times 10^{-3}$ ,  $1.0 \times 10^{-2}$  M, respectively. ( $\lambda_{\text{ex}} = 360$  nm).

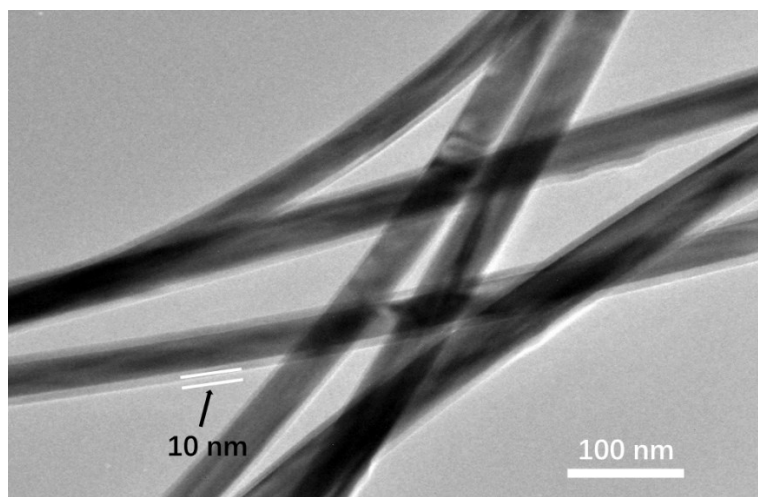


**Fig. S5** The TEM image of AgNWs capped with a PVP layer. The thickness of PVP capping layer (about 10 nm) was clearly observed on the surface of the AgNWs.

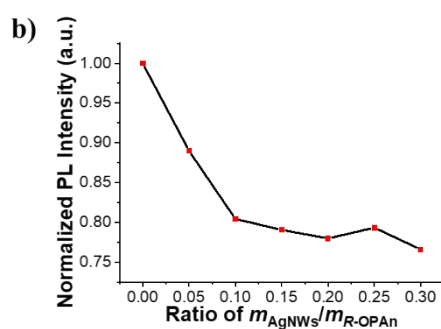
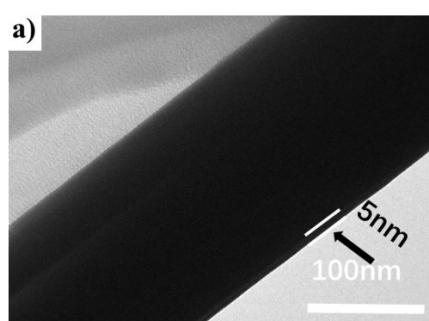


**Fig. S6** (a) The TEM image of AgNWs capped with a PVP layer. The thickness of PVP capping layer (about 5 nm) was clearly observed on the surface of the AgNWs. (b) Fluorescence spectra of R-OPAn-NPs/AgNWs composites with different mass ratios of  $m_{\text{AgNWs}}/m_{\text{R-OPAn}}$  ( $[R\text{-OPAn-NPs}] = 5 \times 10^{-4} \text{ M}$ ,  $\lambda_{\text{ex}} = 360 \text{ nm}$ ).

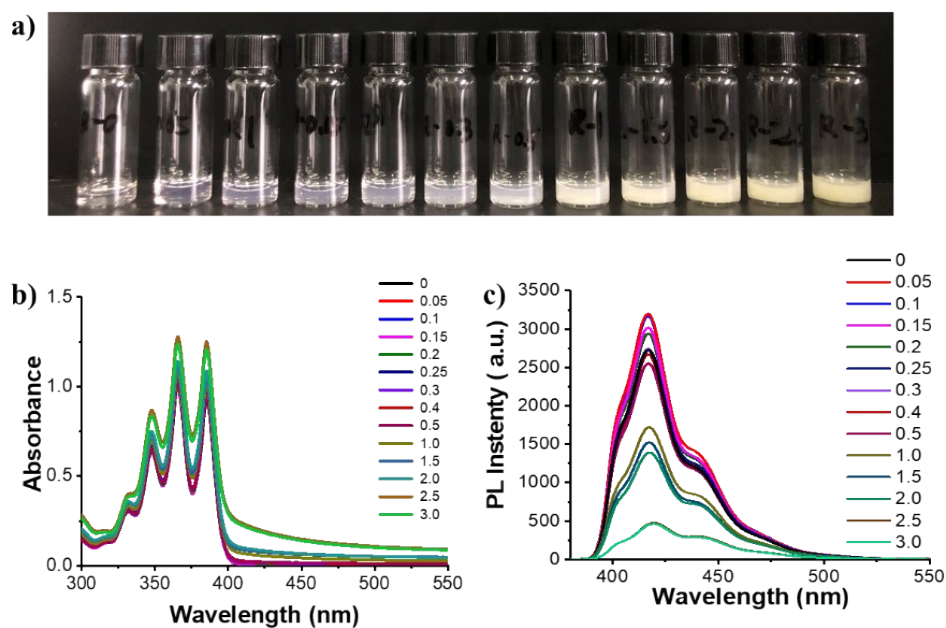


**Fig. S7** (a) The picture of *R*-OPAn-NPs/AgNWs composites of different mass ratios under day light. UV-vis spectra (b) and Fluorescence spectra (c) of *R*-OPAn-NPs/AgNWs composites with different mass ratios of  $m_{\text{AgNWs}}/m_{\text{R-OPAn}}$  ( $[R\text{-OPAn-NPs}] = 5 \times 10^{-4} \text{ M}$ ,  $\lambda_{\text{ex}} = 360 \text{ nm}$ ).

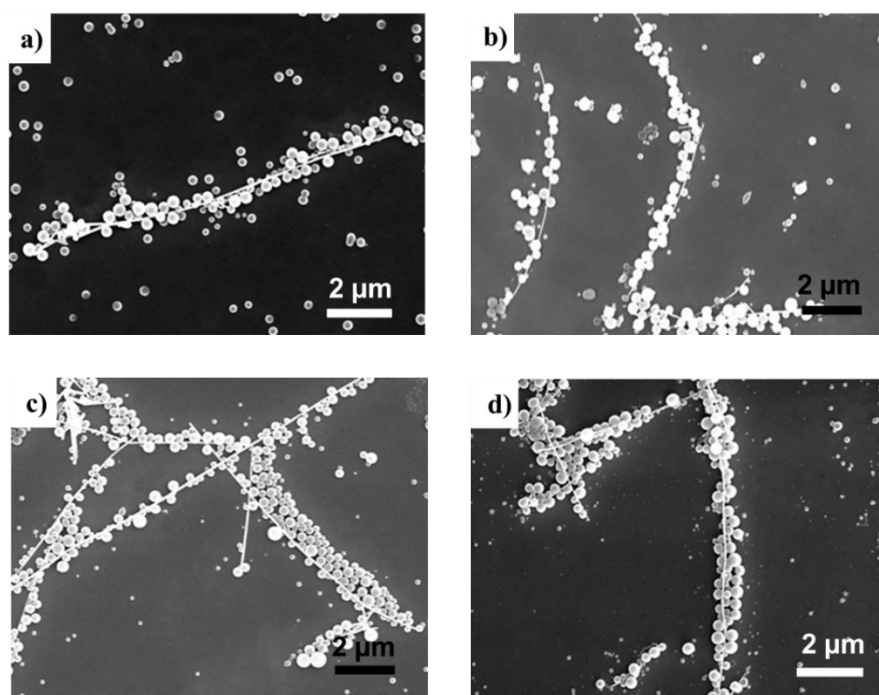


**Fig. S8** (a) ~ (d) The SEM image of *R*-OPAn-NPs/AgNWs composites with different mass ratios of  $m_{\text{AgNWs}}/m_{\text{R-OPAn-NPs}}$ . ( $[R\text{-OPAn-NPs}] = 5 \times 10^{-4} \text{ M}$ ) The corresponding mass ratios of  $m_{\text{AgNWs}}/m_{\text{R-OPAn-NPs}}$  is 0.5, 1.0, 1.5, 2.0.

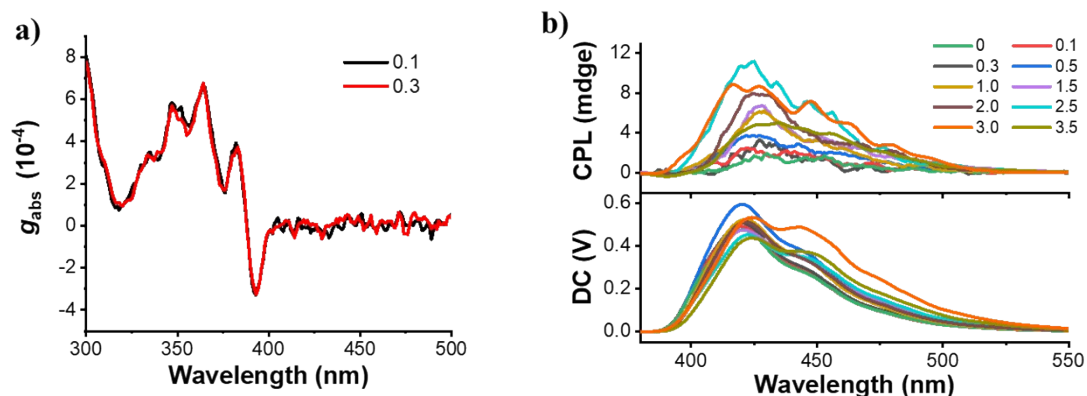


**Fig. S9** (a) Dissymmetry factor  $g_{\text{abs}}$  of *R*-OPAn-NPs/AgNWs composites with different mass ratios ( $m_{\text{AgNWs}}/m_{\text{R-OPAn}} = 0.1, 0.3$ ). (b) CPL spectra of *R*-OPAn-NPs/AgNWs composites with different mass ratios. ( $[R\text{-OPAn-NPs}] = 5 \times 10^{-4} \text{ M}$ ,  $\lambda_{\text{ex}} = 360 \text{ nm}$ ).

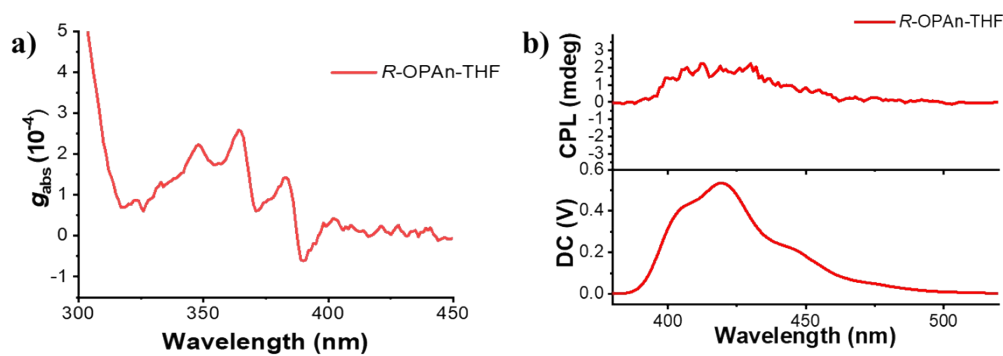


**Fig. S10** Dissymmetry factor  $g_{\text{abs}}$  (a) and CPL spectra (b) of *R*-OPAn dissolved in THF. ( $[R\text{-OPAn}] = 5 \times 10^{-4} \text{ M}$ ,  $\lambda_{\text{ex}} = 360 \text{ nm}$ ).

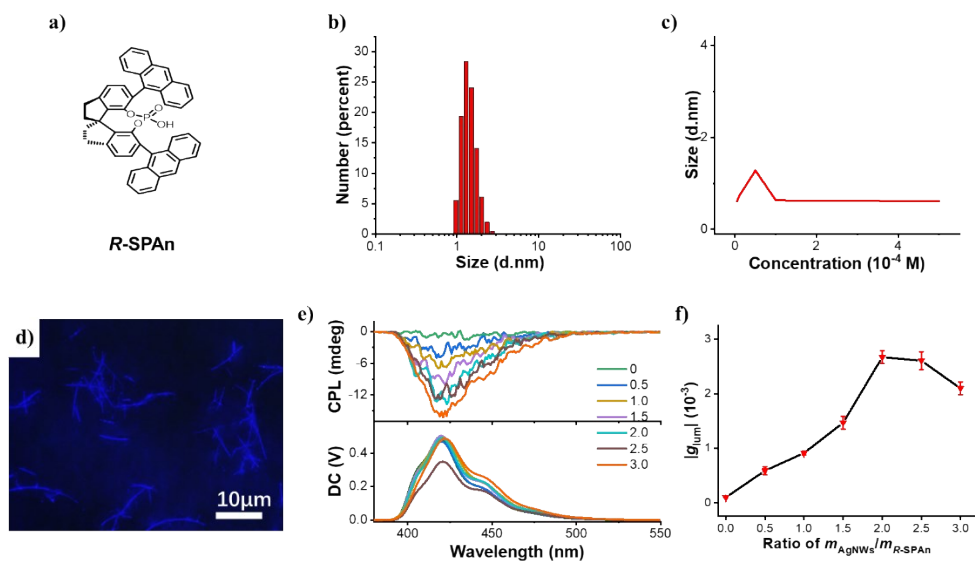


**Fig. S11** (a) The chemical structure of *R*-SPAN. (b) Dynamic light scattering of *R*-SPAN dissolved in ethanol. ( $[R\text{-SPAN}] = 5 \times 10^{-4}$  M). (c) The nanoparticle size of different concentrations of *R*-SPAN in ethanol. ( $[R\text{-SPAN}] = 5 \times 10^{-4}$  M). (d) The fluorescence microscopy of *R*-SPAN/AgNWs composites. ( $\lambda_{\text{ex}} = 325$  to  $375$  nm, filter:  $425$  nm to  $800$  nm.  $[R\text{-SPAN}] = 5 \times 10^{-4}$  M,  $m_{\text{AgNWs}}/m_{\text{R-SPAN}} = 2.0$ ). (e) The CPL spectra of *R*-SPAN/AgNWs composites in different mass ratios of  $m_{\text{AgNWs}}/m_{\text{R-SPAN}}$  dispersed in ethanol. ( $[R\text{-SPAN}] = 5 \times 10^{-4}$  M) (f) Dissymmetry factor  $g_{\text{lum}}$  of *R*-SPAN/AgNWs composites in different mass ratios of *R*-SPAN/AgNWs with error bar. ( $[R\text{-SPAN}] = 5 \times 10^{-4}$  M,  $\lambda_{\text{ex}} = 360$  nm)

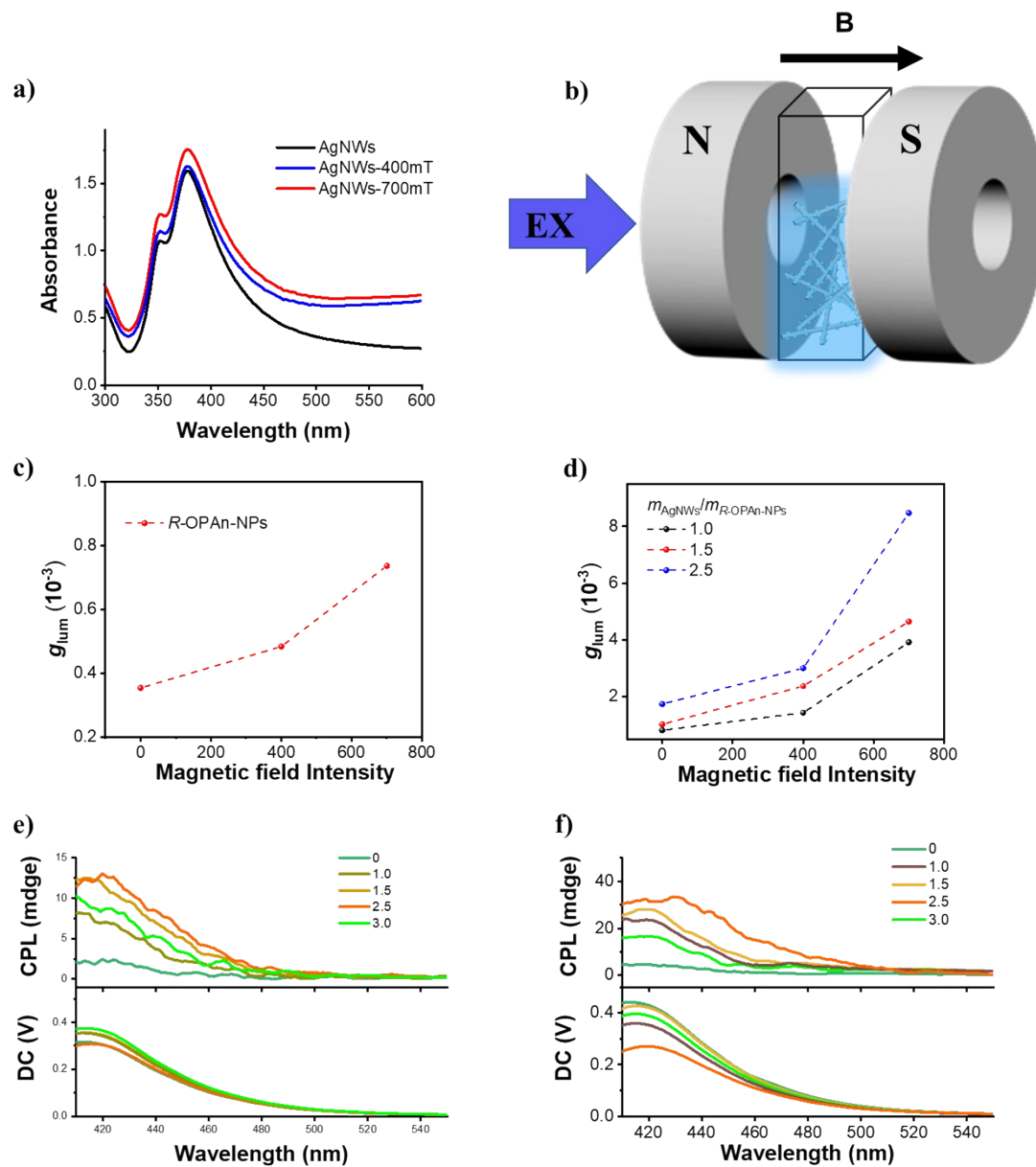


Fig. S12 (a) UV-vis spectra of AgNWs with different external magnetic field. (b) Schematic illustration of the CPL measurement of the R-OPAn-NPs/AgNWs composites with the external magnetic field  $B$ . (c) and (d) the  $g_{lum}$  value of R-OPAn-NPs/AgNWs composites of different mass ratios under the external magnetic field intensity of 0 mT, 400 mT and 700 mT. The CPL spectra of R-OPAn-NPs/AgNWs composites in different mass ratios with external magnetic field (e) 400 mT and (f) 700 mT. ( $[R-OPAn-NPs] = 5 \times 10^{-4} M$ ,  $\lambda_{ex} = 360$  nm).